8

Development of Methane in Earth's Atmosphere

Methane the Gas

Methane molecules have a high capacity to absorpt infrared photons. According to estimates of EPA, the GWP (Global Warming Potential) of methane is 21 times higher than the GWP of carbon dioxide over a 100-year time span. Methane released into the atmosphere ascends to the upper layers of the troposphere where it reacts with ozone, ultimately producing (through chemical reactions) water and carbon dioxide:

$$CH_4 + O_3 + \text{solar radiation} \rightarrow CO_2 + H_2O + H_2 \qquad \text{(Eq. 8.1)}$$

Due to its much lighter molecular weight than that of the other components of the Earth's atmosphere at sea level, hydrogen rises into the stratosphere, whereas, because of their heavier molecular weight, water vapor and methane gas can only rise to the border of the troposphere and stratosphere. The gases involved in Eq. 8.1 absorb infrared radiation from the Sun in different portions of the infrared spectrum (see Figure 9.4). The rate of oxidation of methane in the atmosphere depends on the availability of

the free OH radicals. The estimated life-time of methane, before it breaks down, in the atmosphere (as estimated by IPCC and adapted by the EPA) is in the range of 8 to 12 years. Thus, the effect of the release of methane gas into the atmosphere, is generating additional amounts of CO_2. For every molecule of CH_4 in Earth's atmosphere, 21 molecules of CO_2 are generated. The effect of this additional release of methane into the atmosphere is the equivalent of an additional release of CO_2 which leads to a cooling of the Earth's atmosphere due to the: (1) increased convection within the troposphere and (2) decreased total atmospheric pressure (see Eq. 2.26). Oxidation of methane is a primary source of water vapor in today's upper troposphere. Therefore, methane gas together with the water vapor, help: (1) shield the Earth's surface from the solar irradiation and (2) lower the average surface temperature of the Earth.

Today's major sources of methane entering the atmosphere are shown in the global methane cycle (Figure 8.1): (1) volcanic activity, (2) marshes and tundra, (3) rice paddies, (4) livestock, (5) hydrocarbons, i.e., production

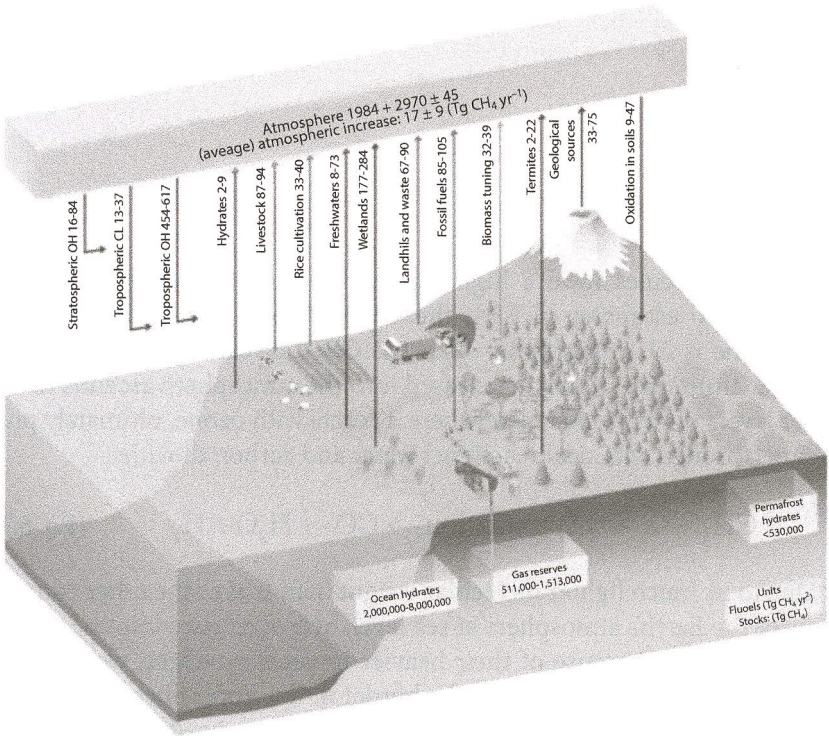

Figure 8.1 Today's global methane cycle. (After Curtis, T., 2015 from C B Dunkerton, as estimated in Ar5; in: Skeptical Science, 2015.)

and burning, (6) natural gas migration to the Earth's surface and (7) landfills and waste. A great volume of methane is released in volcanic eruptions and degassing of the mantle material. Yasamanov (2003) estimated that $\approx 5 \times 10^{15}$ g of CH_4 are released yearly to oceanic water at the spreading zones of mid-ocean ridges. The quantity of methane released to the atmosphere from marshes and tundra is estimated between 5 to 70×10^{13} g annually. From tundra, the amount of CH_4 released is about 4×10^{13} g/year. Enteric fermentation contributes 2 to 20×10^{13} g/year. The total amount of methane released annually into the atmosphere from natural sources is estimated at ≈ 2 to 3×10^{15} g. Methane is also generated because of many human activities. Rice paddies produce about 5×10^{14} g of methane annually. Oil and gas production, burning and related operations add up to 9×10^{14} g of methane annually, which is one order of magnitude lower than the amount of methane released from the natural sources. A great amount of methane is released to the atmosphere because of gas migration to the Earth's surface from coal, oil, and gas deposits and the Earth's mantle (Khilyuk *et al.*, 2000, and Robertson and Chilingar, 2017). The total amount from this latter source is unestimated, although it is likely $\approx 5 \times 10^{15}$ g/year. The burning of fossil fuels contributes 1×10^{13} g/year of methane to the atmosphere.

The content of methane in the atmosphere has been gradually increasing over the last century. Although the methane content constitutes only about 1.8 ppm in the Earth's atmosphere, national and international policy makers have declared the methane gas extremely dangerous to the Earth's climate because of a high potency (about 100 times more potent than CO_2 over the time span of 20 years) of its molecules to absorb the infrared radiation. Together with the growing contents of CO_2 and other greenhouse gases, it is supposedly capable of causing drastic changes in the Earth's climate. According to the conventional anthropogenic theory of global warming, due to the absorption of the infrared radiation by the molecules of the atmosphere, these molecules intercept infrared photons in the lower layer of troposphere, thus warming the Earth. This anthropogenic theory is the basis for strong political and economic actions against further expansion of fracking, e.g., used in the shale-gas production. Additional discussion about the effect of increasing the carbon dioxide content of the Earth's atmosphere shows that increasing the carbon dioxide content will actually lower the Earth's temperature and not increase it as many people erroneously believe (see Chapter 10).

Again, this conventional anthropogenic theory (backed and promoted by IPCC and other national and international organizations over the last 25 years) has been based, without scientific support, solely on the phenomena

of heat transfer in the troposphere as only occurring by radiation, whereas in reality, it is convection and not radiation that is the overwhelming form of heat transfer in the troposphere as documented in Chapter 10. In the troposphere today, heat transfer occurs 67% by convection, 8% by radiation, and 25% by water vapor condensation (Sorokhtin *et al.*, 2007). Moreover, analyzing the postulates in the incorrect conventional theory, it completely ignores the fact that many molecules of the *greenhouse gases* (H_2O, for example) intercept the infrared solar irradiation in the upper layers of stratosphere and not in the troposphere where the methane is located.

Historic Levels of Methane in the Earth's Atmosphere

Methane and ammonia are important trace gases in the Earth's atmosphere. Methane and ammonia were present at the initial stages of the Earth's development (see Figure 5.1). The methane content in the Earth's atmosphere today is 0.00017% (1.7 parts per million by volume). As one of the greenhouse gases of the Earth's atmosphere, methane traps a significant amount of IV radiation. Today's quantity of methane in the atmosphere is the result of a balance between production on the Earth's surface and destruction in the atmosphere. The source of the Earth's methane is: (1) when organic matter decomposes in oxygen-poor environments, e.g., marshes, rice paddies, or the digestive systems of herbivores; (2) from combustion, e.g., burning, of hydrocarbons; and (3) from inorganic reactions (consequently termed abiogenic methane).

Early in the Earth's history, about 3.5 BY ago, there was 1,000 times as much methane in the atmosphere as there is today (see Figure 5.1). The earliest methane that was released into the atmosphere appears to be the result of volcanic activity. The first bacteria contributed methane to the atmosphere by converting hydrogen and carbon dioxide into methane and water.

The emergence of the Precambrian iron ore formations is based on the iron-oxidizing processes by thermal dissociation of the CO_2-saturated oceanic waters and hydration by the same waters of iron-containing oceanic crust rocks. In these processes, methane was also generated:

$$\begin{aligned} &4Fe + 2H_2O + CO_2 \rightarrow 4FeO + CH_4 + 41.8 \text{ kcal/mol} \\ &FeO + 2CO_2 + H_2O \rightarrow Fe(HCO_3)_2 \end{aligned} \qquad \text{(Eq. 8.2)}$$

Today, the mantle does not contain free iron. The methane generation from the oceanic rift zones historically occurred during the hydration of

the oceanic crustal rocks containing bivalent iron, mostly according to the following reactions:

$$4Fe_2SiO_4(\text{fayalite}) + 12Mg_2SiO_4(\text{forsterite}) + 18H_2O + CO_2 \rightarrow$$
$$4Mg_6(SI_4O_{10})(OH)_8(\text{serpentine}) + 4Fe_2O_3(\text{hematite})$$
$$+ CH_4 + 183.4 \text{ kcal/mol.} \qquad \text{(Eq. 8.3)}$$

Due to isotope fractioning between the carbon dioxide and methane, methane was enriched in the light isotope ^{18}C, whereas the heavy isotope ^{13}C mostly migrated to carbon dioxide. Such isotope shifts occur, for instance, in the hydrotherms of the *black smokers* which arise on serpentinites. Methane in such sources usually has $\delta^{13}C \approx -13$ to $-14‰$, whereas the oceanic water-dissolved HCO_3^- and CO_2 have the shifts close to $\delta^{13}C = -5.5‰$ (Sorokhtin *et al.*, 2001). This indicates that the isotopic exchange between carbon dioxide and methane occurs according to the following reaction:

$$^{12}CO_2 + {}^{13}CH_4 \rightarrow {}^{13}CO_2 + {}^{12}CH_4 + 0.412 \text{ kcal/g} \qquad \text{(Eq. 8.4)}$$

in the direction of lowering $\delta^{13}C$ in methane.

As the iron ore formations were highly developed in Precambrian, it is expected that the iron released from the mantle to the hydrosphere, as well as the hydration of the iron silicates occurred as described by Eq. 8.3. This was followed by profuse abiogenic methane generation.

The maximum iron transport to the ocean was accompanied by a maximum methane generation rate. This iron oxide release, in turn, resulted in increasing the mass of the methane-consuming bacteria. The iron oxide release may be described as follows:

$$Fe + H_2O \rightarrow FeO + H_2 + 5.84 \text{ kcal/mol} \qquad \text{(Eq. 8.5)}$$

Fractioning of carbon isotopes always produces a lighter methane isotopic composition, and, hence, a lighter carbon composition in organic matter C_{org} in the bacteria which consumed this methane. This is a likely explanation of the extremely low shifts from $-50‰$ to ≈ -80 $\delta^{13}C_{org}$ in the methane-consuming bacteria. It may also explain local minima in $\delta^{13}C_{org}$ distribution at the time when the largest mass of the iron ore formations was deposited at the end of the Archaean and in the Early Proterozoic time.

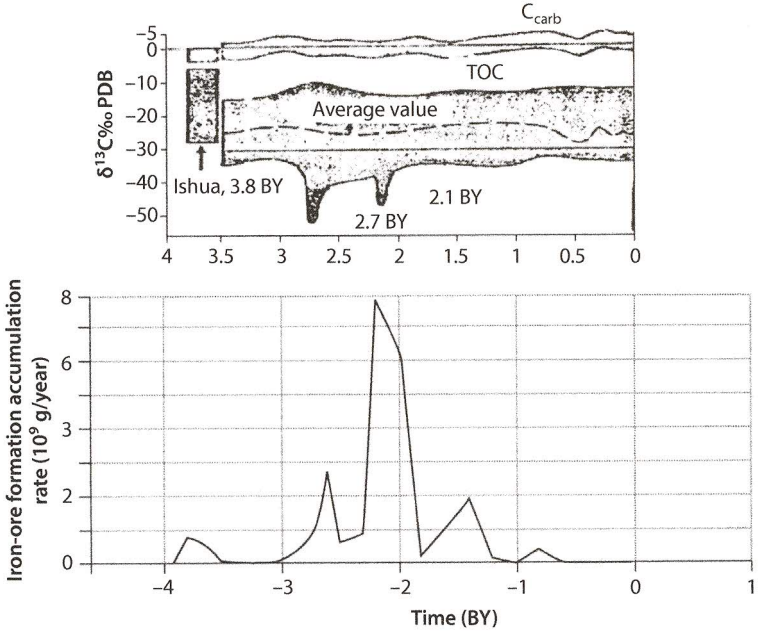

Figure 8.2 Carbon isotopic shifts in organic matter versus epochs of the Precambrian iron-ore formations. Upper diagram: $\delta^{13}C_{org}$ and $\delta^{13}C_{carb}$ distributions in the Earth's evolution (Schidlowski, 1987). Lower diagram. The two most outstanding Precambrian iron-ore formation deposition epochs clearly correspond with the two local minima on the envelop of the minimum $\delta^{13}C_{org}$ values. Unfortunately, the upper diagram does not include their complementary positive $\delta^{13}C_{carb}$ anomalies which reached +8 to +11‰ PDB in the Early Proterozoic time (Semikhatov *et al.*, 1999).

When examining the carbon isotopic shift in organic matter distribution, one can observe the epochs of the massive iron ore deposition on the ocean floor corresponding with a minimum in the organic carbon $\delta^{13}C_{org}$ shift. However, despite a smaller intensity of jaspelite formation rate in the Late Archaean, the $\delta^{13}C_{org}$ isotopic minimum amplitude was the largest at that time.

Every epoch of massive iron ore sedimentation on the ocean floor corresponds to a minimum rate in the Late Archaean time, the $\delta^{13}C_{org}$ isotopic minimum amplitude was the largest. The reason for this may be the existence in the Archaean time, of a high percentage of carbon dioxide in the atmosphere, whereas in the Early Proterozoic time the CO_2 partial pressure had declined, and the rate of methane generation had decreased.

The time iron ore accumulations in the Late Archaean and Early Proterozoic time also corresponds to the two periods of broad stromatolite development (Figure 8.3). Most likely, the nutrition base for the

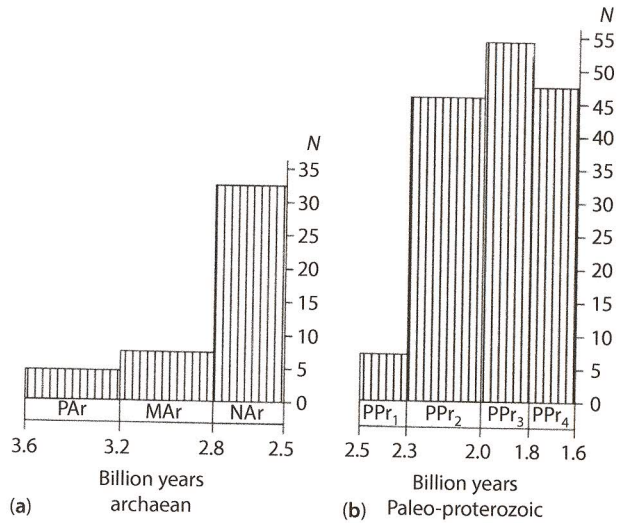

Figure 8.3 Changing of the number of stromatolithic formations in Archaean (a) and Proterozoic (b). (After Semikhatov et al., 1999.) N represents the number of formations with stromatoliths. The Archaean stromatoliths are much smaller in mass than the Early Proterozoic ones ("Paleoproterozoic" by Semikhatov). (After Sorokhtin *et al.*, 2011, p. 455, figure 12.12.)

stromatolites was the abiogenic methane generated in the metallic iron oxidation process according to the reaction of Eq. 8.2 and hydration of the iron silicates according to the reactions like Eq. 8.3.

The abiogenic methane generation rate $\dot{m}(CH_4)$ tends to be controlled by the oceanic crustal formation rate (Dmitriyev *et al.*, 2000; Sorokhtin *et al.*, 2001) equal to $V(H_b + H_{sp})\rho$, where V is the oceanic crustal area increase rate in the rift zones (see Figure 8.4, *Curve 3*); H_b and H_{sp} are, respectively, the oceanic crust's basalt-gabbroid and serpentinite layer thickness; and $\rho \approx 2.9$ g/cm^3. During the epochs of the mass iron ore formation deposition, additional methane release occurred at a rate proportionate to the iron ($\dot{F}$) ore accumulation rate in these formations.

In the Precambrian rift zones, the methane generation occurred due to the hydration of iron silicates under reactions like Eq. 8.3 as well as due to the participation of the free (metallic) iron under reaction Eq. 8.2. Both reactions proceeded within the oceanic crust upon hydration of its rocks by the oceanic water. There is a possibility that similar reactions occurred during the Archaean time because the saturation of the primordial regolite with rain water was saturated with carbon dioxide, as the regolite at that time covered a significant portion of the Earth's surface (see Figures 8.5B, 8.5 C and 8.6).

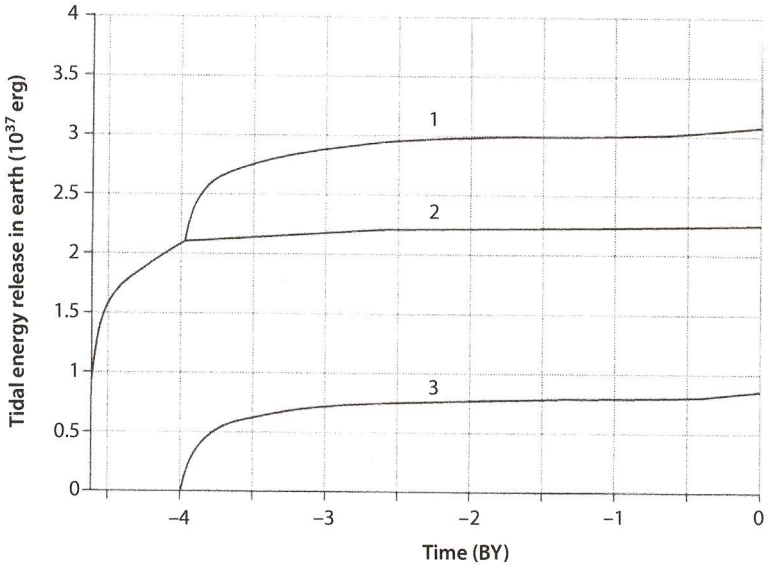

Figure 8.4 Tidal energy release: *Curve 1* – in Earth; *Curve 2* – in mantle; and *Curve 3* – in hydrosphere. (After Sorokhtin *et al.*,2011, fig. 5-10, p. 178.)

Normalizing the calculation results to a single scale can be done by normalizing all methane generation reactions to their unit mass. For example, using the iron oxidization reaction (Eq. 8.2) one mole of methane (16 g) within the rift zones and primordial regolite, forms because of the combination of 304 g of the required reagents to generate this reaction. Thus, the scale factor for this reaction is: $k = 16/304 = 0.0526$. Similarly, the oceanic crust iron-containing rock and regolite hydration reactions are:

$$4Mg_2(SiO_4)(\text{forsetrite}) + 4H_2O + 2(CO_2) \rightarrow$$
$$Mg_6(Si_4O_{10})(OH)_8(\text{serpentine}) + 2Mg(CO_3) + 65.05 \text{ kcal/mol}$$
$$2CaAl_2Si_2O_8(\text{amorite}) + 4H_2O + 2(CO_2) \rightarrow$$
$$A_{l4}(Si_4O_{10})(OH)_8(\text{kaolin}) + 2Ca(CO_3)(\text{calcite}) + 110.54 \text{ kcal/mol.} \quad \text{(Eq. 8.6)}$$

has a scale correction factor, $n = 16/2876 = 0.00556$. The abiogenic methane generation rate, with the excess of CO_2, may be presented as:

$$\frac{d(CH_4)}{dt} = 0.8\times10^{15} U \rho n C_{FeO}(Hsp + 0.12H_b)\left(\frac{S_O}{S_G}\right) + 0.1\,k\left(\frac{d(Fe)}{dt}\right) \quad \text{(Eq. 8.7)}$$

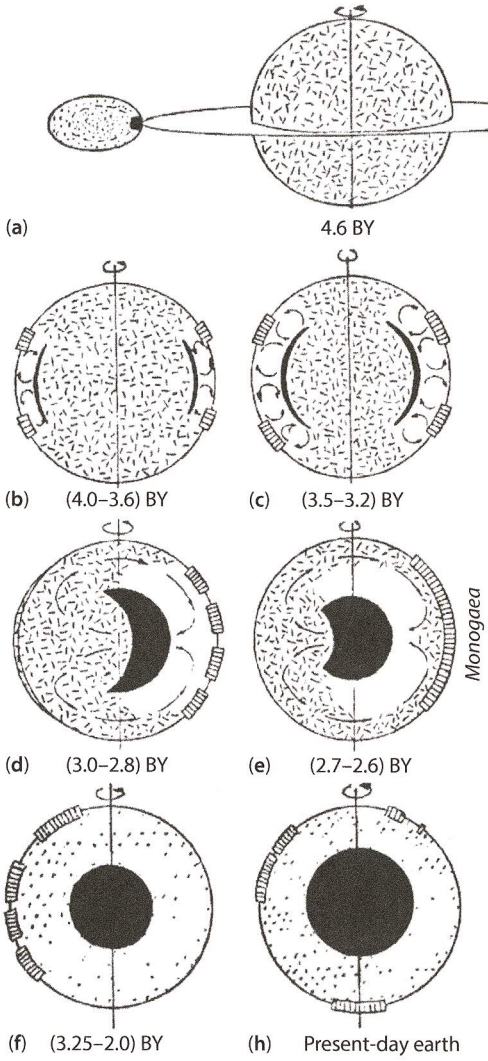

Figure 8.5 Earth structure evolution: (a) the young Earth and moon formation; (b–f) consecutive stages of the Earth's core separation and formation; (g) present-day Earth. The dashes represent the primordial matter; solid black is iron and its oxides melts; white is the Archaean time depleted mantle impoverished in iron, its oxides, and siderophilic elements; the dots are the current-type mantle; and the boxes are continental massifs. (After Sorokhtin *et al.*, 2011, fig. 4.1, p. 117.)

where S_O is the oceanic crustal area (see Figure 8.6); $S_G = 5.1 \times 10^{18}$ cm^2 is the Earth's surface area; C_{FeO} is the ion-oxide concentration in the mantle matter and the oceanic crust (see Figure 8.7); factors 0.1 and 0.8 relate to the recovery extent of a given component ($FeO_2 \cdot FeO$ from the oceanic

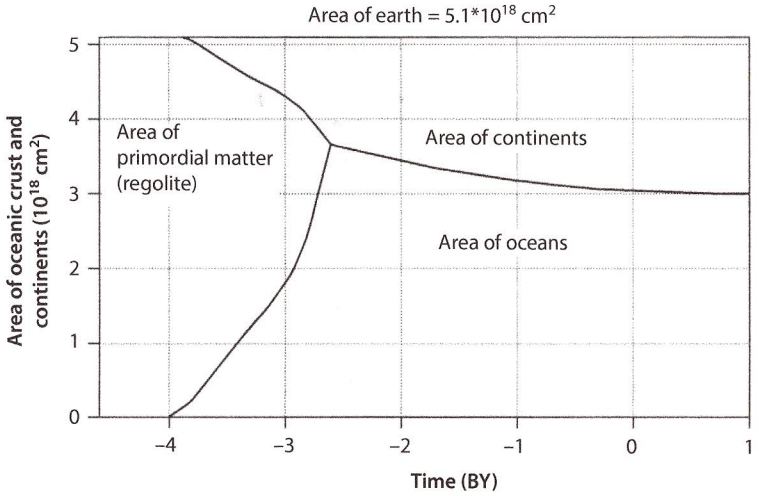

Figure 8.6 Evolution of the areas of the oceans and continents with time. (Sorokhtin *et al.*, 2011, figure 7.4, p. 245.)

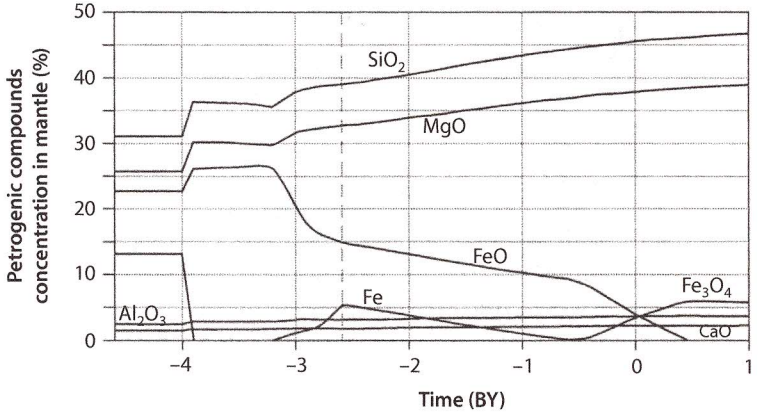

Figure 8.7 Evolution of major petrogenic elements and compounds in the convecting mantle. (After Sorokhtin *et al.*, 2011, figure 4.16, p. 145.)

crust layers). Using Eq. 8.3, the methane generation in today's oceanic crust is 1.86×10^{12} g/year. This is close to the values obtained by Dmitriyev *et al.* (2000) of $\approx 2 \times 10^{6}$ t/year (or 2×10^{12} g/year). The calculated results can be compared with organic carbon isotopic shifts in Figure 8.8. The Precambrian iron ore deposition and methane accumulation clearly correspond to the two minima on the envelope of the minimum $\delta^{13}C_{org}$ values.

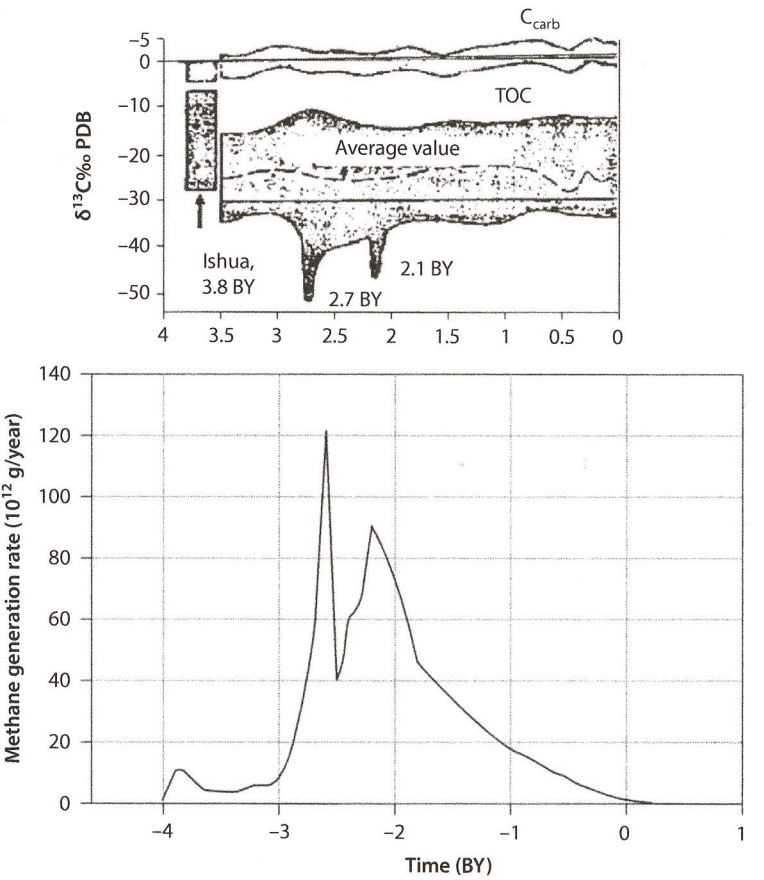

Figure 8.8 Abiogenic methane generation in the oceanic crust plotted using Eq. 8.7 compared with the carbon isotopic shifts in organic matter. Upper diagram: $\delta^{13}C_{org}$ and $\delta^{13}C_{carb}$ distributions versus time (Schidlowski, 1987); lower diagram: abiogenic methane generation rate. Two most outstanding Precambrian iron-ore formation deposition and methane accumulation epochs clearly correspond with the two local minima on the envelop of the minimum $\delta^{13}C_{org}$ values. (After Sorokhtin *et al.*, 2011, figure 12.11, p. 456.)

As shown in Figure 8.8, the generation of abiogenic methane in the oceanic crust ≈4 BY ago, reached 10 million tons per year, and then rapidly declined to a few million tons per year in the Mid-Archaean time. Later, due to the beginning of the Earth's core separation (see Figure 8.5D and 8.5E) and a significant increase in the tectonic activity (see Figure 5.2), the generation of methane (see Figure 8.8) significantly increased and by the end of the Archaean time reached maximum value of about 120 million

tons per year. During the Archaean and Proterozoic time, tectonic activity diminished significantly along with methane generation (≈40 million tons per year). Massive deposition of iron ore formations began in the Early Proterozoic (≈2.2 BY ago) as indicated (Fe) in Figure 8.7. This resulted in renewed intensification of methane generation of ≈90 million tons per year. Subsequently, the abiogenic methane formation gradually decreased to today's rate of 1.8 million t/year. This process will stop in ≈600 million years, when, due to the Earth's core separation process, the mantle becomes totally devoid of bivalent iron.

There is a strong correlation between the organic carbon isotopic shift and methane generation rate. As a result, there are massive Early Precambrian iron ore formations. This is logical as iron oxidizing under the reaction of Eq. 8.2, and its further accumulation in iron ore formations, is accompanied by generation of the abiogenic methane.

Inasmuch as methane is the nutrition base for the cyanobacteria and methane-consuming bacteria, it left noticeable traces in the geological record. Due to carbon isotope fractionation in the exchange reactions between carbon dioxide and methane according to the following reaction:

$$^{12}CO_2 + {}^{13}CH_4 \rightarrow {}^{13}CO_2 + {}^{12}CH_4 + 0.412\ \text{kcal/g}(CH_2) \qquad \text{(Eq. 8.8)}$$

This shows that methane is always enriched in the light carbon isotope. The remaining carbon dioxide later migrates to the carbonates to became isotopically heavier. For that reason, organic matter formed from methane-consuming bacteria will always have a lighter carbon isotope composition, sometimes as low as $\delta^{13}C_{org} \approx -50^{o}/_{oo}$ and lower.

This phenomenon may have been the cause of the local $\delta^{13}C_{org}$ distribution minima exactly at the times when the iron ore formations were deposited at the end of the Archaean time and Early Proterozoic time at the greatest rate.

Accelerated methane generation during the deposition of the massive iron ore formations must have affected the evolution intensity of stromatolites (Figure 8.3), which are the remains of laminated bacterial mates (films). If so, a noticeable fraction of these films was formed by methane-consuming bacteria. The bloom of these life forms must have occurred during the massive deposition of the iron ore formations and profuse methane generation. Semikhatov *et al.* (1999) indicated that this time interval is marked by a burst in the growth of stromatolite buildups (see Figures 8.3 and 8.8).

A portion of the abiogenic methane could have concentrated in accumulations of oceanic deposits of gas-hydrates. Massive shungite deposition occurred in Karelia during the Late Jatulian time (the second half of Early

Proterozoic time). The shungites are coaly matter that are likely graphitized remains of previous hydrocarbon accumulations.

Beside the generation of methane in the oceanic rift zones, a nonrecurring abiogenic methane release into the atmosphere occurred at the beginning of Archaean time due to the hydration of the ultramafic regolith still covering most of the planet (see Figures 8.5B, 8.5C and 8.6). The methane release intensity may be estimated by assuming that over a period of 100 MY, from ≈4.0 to 3.9 BY ago, the Earth's entire primordial layer of regolith was soaked with rainwater containing carbon dioxide. The initial iron concentration of the regolith was ≈13%, and its oxides, ≈23%. In this situation, with the excess of CO_2 in the water, the original atmospheric methane pressure may be determined as:

$$p_{(CH_4)} = p_r h_r (0.13k + 0.23n)\left(\frac{S_r}{10^3 S_G}\right) \qquad \text{(Eq. 8.9)}$$

where the regolith density (by analogy with the lunar regolith) is $p_r \approx 2$ g/cm^2; h_r is the unknown thickness of the rainwater-soaked regolith layer; *Sr* is the area covered by the regolith (see Figure 8.6); $S_G = 5.1 \times 10^{18}$ cm^2 is the Earth's area. In the methane formation reactions (Eq. 8.2 and Eq. 8.3), the limiting factor is the mass of the degassed carbon dioxide. The authors estimate that by the time 3.9 BY ago, $m(CO_2) \approx 6.4 \times 10^{20}$ g of carbon dioxide was degassed from the mantle. With the assumption that all this gas was spent for methane generation, its mass would then be $m(CH_4) \approx m(CO_2) \times 16/44 \approx 2.33 \times 10^{20}$ g, and its partial pressure would not exceed $p_{(CH4)} \approx 46$ mbar. This methane pressure calculated using Eq. 8.9 corresponds to a carbon dioxide rainwater-soaked regolith layer of 37.5-m thick. The $p_{(CH4)}$ estimate appears to be maximal. The actual methane partial pressure at the beginning of Archaean time was lower, but most likely no lower than 20 mbar.

Methane could not accumulate in the sea basin water in the locations where it was generated (within the primordial regolith and outside the sediment sequences). Thus, it was released directly into the atmosphere making the Earth's atmosphere very reducing. Therefore, the atmosphere at the beginning of the Early Archaean time was significantly reducing and the atmosphere's composition was carbon dioxide-nitrogen-methane. Subsequently, in about 100 MY after the total hydration of the primordial regolith, the Archaean atmosphere's reducing potential must have declined due to methane photodissociation by solar radiation with the formation of formaldehyde:

$$CH_4 + CO_2 + h\nu \rightarrow 2HCOH(\text{formaldehyde}). \qquad \text{(Eq. 8.10)}$$

Besides, being affected by the solar ultraviolet (UV) radiation, methane was also oxidized in the humid and warm Early Archaean atmosphere according to the following reaction:

$$CH_4 + H_2O + h\nu \rightarrow CO + 3H_2, \qquad \text{(Eq. 8.11)}$$

with the hydrogen evaporating. Therefore, the Earth's Archaean atmosphere became a carbon dioxide-nitrogen one, with a minor methane content and at the equilibrium humidity content.

As Galimov (2001) has shown, for life to have emerged abiogenically, some simple source organic compounds had to have first accumulated. One such compound may have been formaldehyde, which as methane formed during the iron oxidation:

$$2Fe + H_2O + CO_2 \rightarrow 2FeO + HCOH(\text{formaldehyde}) + 3.05 \text{ kcal/mol.} \qquad \text{(Eq. 8.12)}$$

Beside the formaldehyde, because of the thunderstorm discharges in the Earth's Early Archaean reducing atmosphere, with its nitrogen and methane composition, another *link* in the chain of primary life, the hydrogen cyanide, must have emerged:

$$N_2 + 2CH_4 + Q \rightarrow 2HCN(\text{hydrogen cyanide}) + 3H_2 \qquad \text{(Eq. 8.13)}$$

where $Q = 26.6$ kcal/ mol is the part of the thunderstorm discharge energy absorbed by the Eq. 8.13 reaction. Early in the Archaean time (≈3.9 BY ago) bacteria probably had not yet emerged. If so, the isotopic shifts in organic matter at that time were determined only by the properties of the reactions like Eq. 8.2 and 8.3 with no addition of isotopic shifts due to the bacterial metabolism. Apparently, these oldest Earth's rocks were populated by bacteria only somewhat later and with no participation of the abiogenic methane. That may be one reason why the carbon isotopic ratios about 3.9 to 3.8 BY ago in the Shidlovsky diagram have slightly elevated $\delta^{13}C$ values when compared to subsequent epochs (see Figures 8.2 and 8.8).

The evolution of abiogenic methane partial pressure in the atmosphere was developed by the authors using Eqs. 8.1 and 8.8 with results are presented in Figure 8.9. To make the characterization of the methane generation on Earth more complete, Eq. 8.8 must be amended by: (1) the addition of swamp methane in northern Eurasia and Canada, (2) methane generated

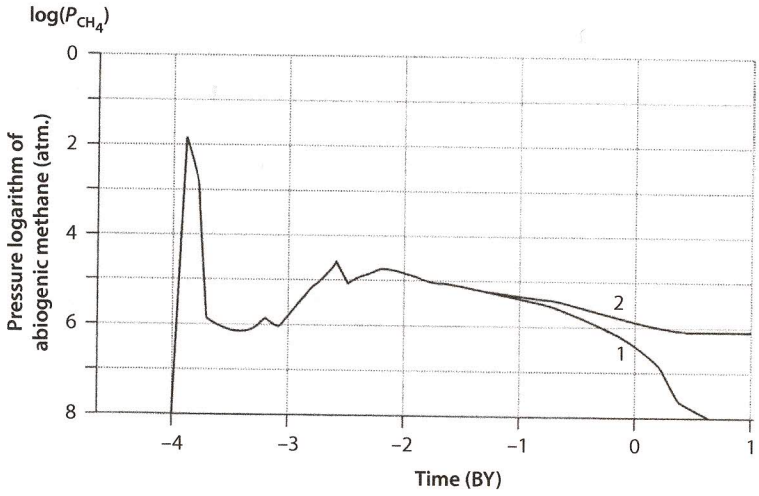

Figure 8.9 Atmospheric methane partial pressure versus time: *Curve 1* – methane generation in the oceanic crust and *Curve 2* – total methane generation in the oceanic crust and on the continents. (After Sorokhtin *et al.*, 2011, figure 12.14, p. 459.)

by soil-bacteria in the humid tropical areas, and (3) methane seeping up from the continental hydrocarbon accumulations.

It is assumed that the process of evolution of partial pressure of methane began about 1.8 BY ago. Today, Earth's atmospheric methane partial pressure is $p_0 \approx 1.216 \times 10^{-6}$ bar ($\log p_0 \approx -5.92$). Thus, one can calculate the total methane partial pressure in the Earth's atmosphere. The authors estimate is that today's methane generation on the continents is 3.3 times that generated by the oceanic crust. The methane partial pressure has fluctuated during the Earth's evolution by at least four orders of magnitude (Figure 8.9).

Methane is an unstable hydrocarbon gas and under normal circumstances rapidly decomposes. For example, the dissolved gas from the oceanic water: (1) escapes into the atmosphere; (2) rises to the stratosphere; (3) rapidly decomposes when it encounters hard solar radiation and breaks down into carbon dioxide; and (4) remains within the atmosphere as carbon dioxide:

$$CH_4 + 2H_2O + hv \rightarrow CO_2 + 4H_2 \qquad \text{(Eq. 8.14)}$$

$$CH_4 + 2OH + hv \rightarrow CO_2 + 3H_2 \qquad \text{(Eq. 8.15)}$$

Within the oceanic water, methane is consumed by bacteria and then released as a carbon dioxide gas byproduct. Also, when the bacteria die, their organic material breaks down into heat, carbon dioxide and water:

$$CH_4 + \text{bacteria} \rightarrow CO_2 + (\text{OM}). \qquad \text{(Eq. 8.16)}$$

In the Early Precambrian active metamorphism zones, the direct reduction of methane to carbon occurred with the formation of coaly matter (combustible shales, shungite and even graphite). In the late Precambrian, especially in the Phanerozoic time, direct methane oxidation occurred:

$$CH_4 + 4O_2 \rightarrow 2H_2O + CO_2 + 131.2 \text{ kcal/mol}. \qquad \text{(Eq. 8.17)}$$

Despite all these losses, the methane remaining in the sedimentary sequences, especially in the absence of oxygen, could form hydrocarbon accumulations, including gas hydrates. More complex hydrocarbons were also formed from the methane. Lein and colleagues (1998, 2000) believe that the *black smoker* sulfide ores are a unique target for studying genesis of organic matter. The chemical peculiarity of hydrothermal systems which include dissolved H_2, H_2S, CH_4, NH_4, Fe^{2+}, Mn_2^+, CO, CO_2, the NaCl electrolyte, and sulfide minerals as a solid phase (electrodes) gives rise to a possibility of organic compound bacterial synthesis on the sulfide mineral matrix in this giant electrochemical cell. Lein *et al.* (1998) studied lipid fractions in hydrothermal springs using single-dimensional and bi-dimensional chromatography and noted that all similar samples included a broad range of neutral lipids and phospholipids, and that in the water-methanol medium, proteins and DNAs.

Mass-spectrometric analysis of the lipid fractions from the organic matter in sulfide ores confirms the presence of biogenic components, including cellular material of microorganisms. Fatty acids from the present-day sulfide ores are compositionally close to lipids from the biomass of chemoautotroph bacteria within the hydrothermal community in the active fields of mid-ocean ridges (Lein *et al.*, 1998; Lein and Sagalevich, 2000; Perisypkin *et al.*, 1998).

Monitoring of Methane Gas Emissions

Rossenfoss (2015), in an excellent article, discussed the need for better monitoring of methane gas emissions. According to the EPA, the natural gas emissions would rise by 25% by 2025 without further action.

According to the EPA, since 1990, the industries' natural gas emissions are down by 16%. Rossenfoss (2015) stated that this was mainly due to: (1) reduced emissions from controlled devices, (2) installation of plunger lift systems, and (3) green well-completion methods, which capture gas that once escaped from the fluids, flowing back after fracturing.

Based on the study done by the consulting firm ICF (commissioned by EDF), the added cost, using available technology, of a 40% reduction in emissions from natural gas production processing and delivery system would be about 1 cent per MCF produced.

Rossenfoss (2015) showed that great strides have been made by oil/gas companies in the field of emission control. The conclusion was that operators should regularly monitor and maintain their gas-producing wells and equipment.